




## RESEARCH ARTICLE

# An Intraoperative Trajectory-Determined Strategy of Patient-Specific Drill Template for C<sub>2</sub> Transoral Pedicle Insertion in Incomplete Reduction of Atlantoaxial Dislocation: An *In Vitro* Study

Jing Shan, MD<sup>1</sup>, Mei-song Zhu, MD<sup>1</sup> , Lu-tao Li, MD<sup>2</sup>, Peng Peng, MD<sup>3</sup>, Min Dai, MD<sup>1</sup>, Li-jun Lin, MD<sup>2</sup> , Jian-yi Li, MD<sup>4,5</sup> 

<sup>1</sup>Department of Orthopaedics, Artificial Joints Engineering and Technology Research Center of Jiangxi Province, The First Affiliated Hospital of Nanchang University, Nanchang, Department of <sup>2</sup>Joint and Orthopaedics, Zhujiang Hospital and <sup>4</sup>Anatomy, Guangdong Provincial Key Laboratory of Medical Biomechanics, School of Basic Medical Sciences, Southern Medical University and <sup>3</sup>Department of Orthopaedics, TCM-Integrated Hospital of Southern Medical University, Guangzhou and <sup>5</sup>Nanhai Hospital, Southern Medical University, Foshan, China

**Objectives:** This study aims to explore a novel intraoperative trajectory-determined strategy of grouped patient-specific drill templates (PDTs) for transoral C<sub>2</sub> pedicle screw insertion (C<sub>2</sub>TOPI) for atlantoaxial dislocation (AAD) with incomplete reduction and to evaluate its efficiency and accuracy.

**Methods:** Ten cadaveric C<sub>2</sub> specimens were scanned by computed tomography (CT) and randomly divided into two groups (the PDT and freehand groups). A novel intraoperative trajectory-determined strategy of grouped PDTs was created for AAD with incomplete reduction. C<sub>2</sub>TOPI was performed by use of the PDT technique and the fluoroscopy-guided freehand technique. After surgery, the screw deviations from the centroid of the cross-section at the midpoint of the pedicle and screw position grades were assessed in both groups.

**Results:** Compared to the freehand group, the PDT group had a significantly shorter surgery time than the freehand group (47.7 vs 61.9 min,  $P < 0.001$ ). The absolute deviations from the centroids between the preoperative designs and postoperative measurements on the axial plane of the pedicle were  $1.19 \pm 0.25$  mm in the PDT group and  $1.82 \pm 0.51$  mm in the freehand group. On the sagittal plane of the pedicle, the corresponding values were  $1.10 \pm 0.33$  mm in the PDT group and  $1.70 \pm 0.49$  mm in the freehand group. The absolute deviations of the freehand group on both the axial and sagittal planes were higher than that of the freehand group ( $P < 0.05$  and  $P < 0.05$ , respectively). For the grade of screw insertion position, nine (90%) were observed in type I and one (10%) in type II in

**Address for correspondence** Min Dai, MD, Department of Orthopaedics, Artificial Joints Engineering and Technology Research Center of Jiangxi Province, The First Affiliated Hospital of Nanchang University, 17 yongwaizheng street, Donghu District, Nanchang, Jiangxi, China 330006 Tel: +15079093645; Fax: +86-791-88623153. Email: daiminyisheng@163.com; Li-jun Lin, MD, Department of Orthopaedics, Zhujiang Hospital, Southern Medical University, 253 Gongye Street, Haizhu District, Guangzhou, Guangdong, China 510280 Tel: +13822153869; Fax: +86-020-61643888. Email: gost1@smu.edu.cn

Jian-yi Li, MD, Department of Anatomy, Guangdong Provincial Key Laboratory of Medical Biomechanics, School of Basic Medical Sciences, Southern Medical University, 1023 Shatai Nan Road, Baiyun District, Guangzhou, Guangdong, China

Nanhai Hospital, Southern Medical University, 28 Liguan Road, Lishui Town, Nanhai District, Foshan, Guangdong, China 510515 Tel: +18665000205; Fax: +86-020-62789091. Email: lijianyi@outlook.com

Jing Shan, Meisong Zhu and Lutao Li contributed equally to this work

**Grant Sources:** This work is partly supported by the National Natural Science Foundation of China (31771330), National Key Research and Development Program of China (2017YFC0110602), and Guangdong and Guangzhou Provincial Scientific and Technique Program (2014A020212200, 2015A040404022, 2015B010125006, 2015B010125005, 201704020129, and 201704020069). No benefits in any form have been or will be received from a commercial party related directly or indirectly to the subject of this manuscript.

**Disclosure:** The authors declare that they have no conflict of interest.

All authors listed meet the authorship criteria according to the latest guidelines of the International Committee of Medical Journal Editors, and are in agreement with the manuscript.

Received 21 October 2020; accepted 17 April 2021

the PDT group, whereas five (50%) were in type I, three (30%) were in type II, and two (20%) in type III in the freehand group. Statistical differences could not be found between the groups in terms of the screw positions ( $P > 0.05$ ).

**Conclusion:** The novel intraoperative trajectory-determined strategy of grouped PDTs can be used as an accurate and feasible method for C<sub>2</sub>TOPI for AAD with incomplete reduction.

**Key words:** Atlantoaxial joint; Pedicle screw; 3D printing; Cadaver; Classification

## Introduction

Atlantoaxial dislocation (AAD) can cause neck pain, limitations in neck movement, or spinal cord compression. Thus, surgical intervention is usually needed to relieve spinal compression and restore stability between the atlas and the axis in patients<sup>1,2</sup>. In recent years, a specially designed reduction, described as transoral atlantoaxial reduction plate (TARP) surgery, has been widely confirmed to be an advanced treatment for AAD<sup>1,3-5</sup> that could allow transoral release, reduction, internal fixation, and bone grafting in a one-stage operation. Transoral C<sub>2</sub> pedicle fixation was introduced in the third generation of the TARP system<sup>6</sup>, which could effectively provide better biomechanical performance than intravertebral insertion fixation. Generally, transoral C<sub>2</sub> pedicle screw insertion (C<sub>2</sub>TOPI) is considered risky because it is proximal to the vital structures such as the vertebral arteries, the spinal cord, and the nerve roots<sup>7</sup>. Therefore, accurate C<sub>2</sub>TOPI is the key to successful clinical application of the TARP system.

Various strategies have been developed for safe and accurate screw insertion in C<sub>2</sub>TOPI. Anatomical free-hand technique was routinely used in clinical practice; however, high perforation incidences from 15% to 17.3% were reported<sup>8-10</sup>. C-arm fluoroscopy which could provide detailed information of the spinal anatomy was thus introduced to facilitate C<sub>2</sub>TOPI<sup>11,12</sup>. However, the overlapping images are not sufficient for atlantoaxial complexity and therefore cannot indicate the screw position accurately<sup>13</sup>. Li *et al.*<sup>14</sup> found that the medial and lateral cortical breach rate of C<sub>2</sub>TOPI was as high as 46.9% performed by the fluoroscopic-guided freehand technique. The recent development of intraoperative three-dimensional (3D) fluoroscopy-based or computed tomography (CT)-based navigation could provide accurate 3D images of the spinal anatomy that could be used for precise pedicle screw placement<sup>13,15,16</sup>. However, these devices are relatively expensive, as well as the operative procedures being complicated and time-consuming, which influences their wide application in clinical trials<sup>13,17</sup>. Patient specific drill templates (PDTs) produced by 3D printing were then introduced to assist C<sub>2</sub>TOPI, which have been confirmed to improve the accuracy and efficacy of C<sub>2</sub>TOPI as well as obviate complex equipment and time-consuming procedures<sup>18,19</sup>. However, these strategies used for PDTs were mainly based on the pre-set trajectory, which could not meet the demands for all kinds of intraoperative reduction in AAD.

Actually, there are two cases of intraoperative reduction of AAD—complete and incomplete reductions<sup>1,4</sup>—which

require different strategies for PDT design. For AAD with complete reduction, surgeons need the optimal trajectories of C<sub>2</sub>TOPI, and the aforementioned traditional PDT strategy that determines the trajectories preoperatively might fulfill these demands. However, for AAD with incomplete reduction, because the C<sub>2</sub>TOPI trajectories would be determined after the intraoperative reduction, the traditional PDT approach may not meet the demands. Thus, a novel PDT approach remains to be developed. Therefore, in this study, we aimed to (i) develop a novel intraoperative trajectory-determined strategy of grouped PDTs specifically for incomplete reduction of AAD and evaluate the (ii) efficiency and (iii) accuracy of this technique in facilitating C<sub>2</sub>TOPI. We hypothesized that this grouped PDT might be an alternative to the fluoroscopy-guided freehand technique for C<sub>2</sub>TOPI.

## Materials and Methods

### Specimens

A total of 10 formalin-preserved cadaveric cervical spines from 10 cadavers (five males and five females aged from 50 to 67 years, with a mean age of 61 years) were harvested and scanned by CT (Philips, Eindhoven, The Netherlands). All cervical vertebrae that fulfilled the following inclusion criteria were included in the study: no bone defects or fractures according to the CT scan images. The CT data were saved in the DICOM (Digital Imaging and Communications in Medicine) format at 0.625 mm intervals with a pixel size of 0.55 mm. Twenty sides of the cadaveric cervical spines were then randomized to undergo C<sub>2</sub>TOPI surgeries through either the PDT technique or the fluoroscopy-guided freehand technique. The PDT design and accuracy assessment were performed by a postgraduate student; the C<sub>2</sub>TOPI surgeries were performed by another attending spinal surgeon. Neither knew whether the specimens belonged to the PDT or freehand group. All specimens underwent internal atlantoaxial fixations with the fourth generation of the TARP system, which added vertebral body screws (VBSs) for fixation based on the third generation of the TARP system<sup>1</sup>.

### Determination of the Centroid at the C<sub>2</sub> Pedicle

All specimens were handled by the same procedures in our previously published protocols<sup>18</sup>. The CT data were imported into Mimics software version 14.11 (Materialize Corp., Leuven, Belgium) to obtain 3D reconstruction models of the C<sub>1</sub> and C<sub>2</sub> vertebrae. The 3D model of C<sub>2</sub> was then exported to

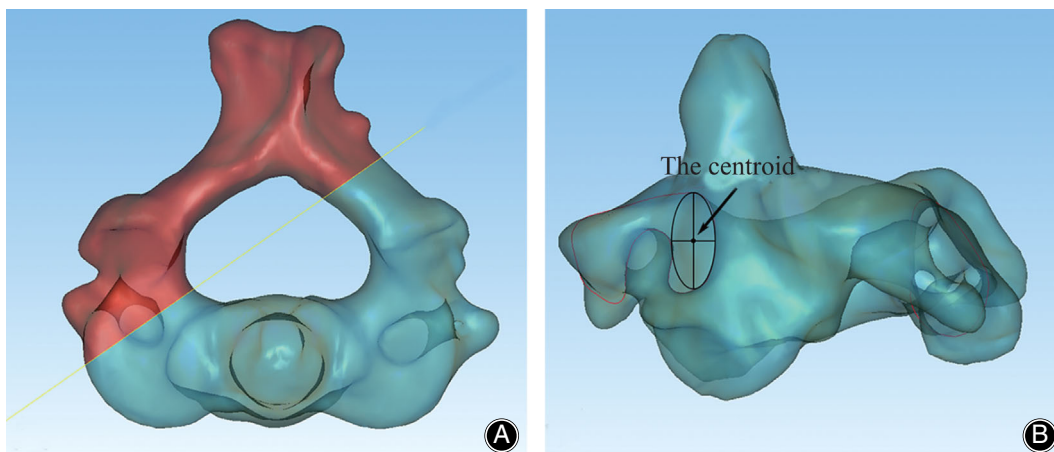


**Fig. 1** Calculation of the centroid of the cross-section at the midpoint of the pedicle of C<sub>2</sub>. (A) The midpoint and corresponding cross-section of each pedicle were determined. (B) After the contour of the cross section was fitted by a maximum ellipse, the centroid was calculated from the maximum ellipse (reprinted from our previous research<sup>18</sup> with permission from Copyright Clearance Center).

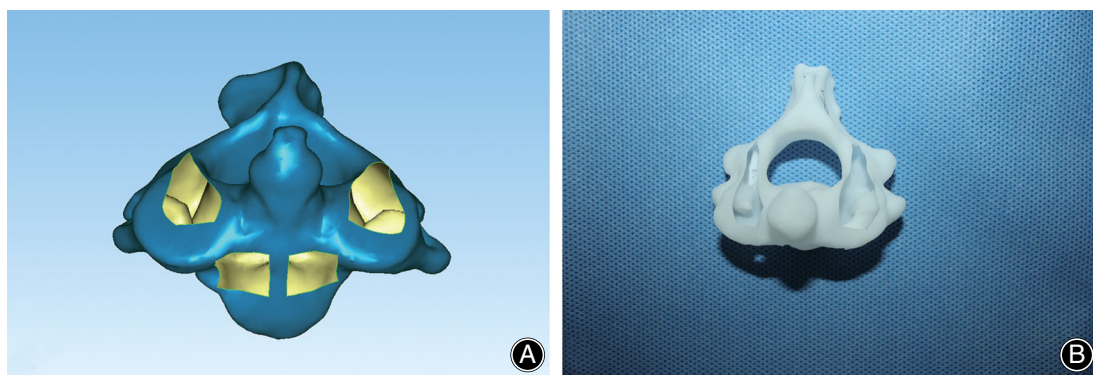


**Fig. 2** 3D model of the C<sub>2</sub> vertebra. (A) 3D C<sub>2</sub> model in which the surfaces of the upper pedicle and anterior vertebral body were removed. (B) 3D-printed model.

Geomagic Studio software version 11.0 (3D Systems Corp, Morrisville, NC) in STL format. The midpoint and corresponding cross section of each pedicle were determined using this software. After the contour of the cross section was fitted by a maximum ellipse, the centroid of the cross section at the midpoint of the pedicle was subsequently calculated from the maximum ellipse (Fig. 1).

#### **Design and Manufacture of Grouped PDTs for AAD with Incomplete Reduction**

A novel intraoperative trajectory-determined strategy of grouped PDTs for C<sub>2</sub>TOPI was developed for AAD with incomplete reduction. The C<sub>2</sub> 3D models were further handled through Geomagic Studio 11.0 software, in which the upper surface of the pedicle and the anterior surface of the vertebral body were removed. Then, the C<sub>2</sub> shell model was extracted and subsequently 3D printed by a RS6000 stereolithography printer (Shanghai Union Technology Corp, Shanghai, China). The structures of the 3D-printed C<sub>2</sub>

models exposed the inner wall of the vertebral artery and the lateral wall of the vertebral canal, which clearly showed the insertion position of the K-wire in the pedicle when it was inserted from the anterior aspect of C<sub>2</sub> (Fig. 2).

The 3D models of C<sub>1</sub>, C<sub>2</sub>, and the TARP were also imported into SolidWorks 2014 (Dassault Systemes, France), in which the PDTs were designed. There were three PDT parts for C<sub>2</sub>TOPI: PDT C, D, and E (Fig. 3A). PDT C was used to guide the holes for temporary reduction screw (TRS) and setscrew, and had a bottom surface and two guide tubes. The bottom surface was the reverse surface of the anterior surface of the vertebral body, by which PDT C could tightly attach to C<sub>2</sub>. The two guide tubes were perpendicular to the bottom surface, and the guide tube that was used to guide for the setscrew was 5 mm higher than that for the TRS. PDT D was designed to fit the TARP surface and was used to locate the intraoperative position of the TARP after atlantoaxial reduction. The inferior two holes were positioned in accordance with the inferior two holes of the

TARP, which were used to screw in VBS. The upper two holes of PDT D were used to determine the entrances of the trajectories. PDT E was used for C<sub>2</sub>TOPI drilling. Since the most areas of the anterior surface of C<sub>2</sub> were covered by the

TARP in the operative procedure, a special “table” structure was designed. The bottom surfaces of the columns under the table and two short pins were aligned to the TARP-uncovered surface of C<sub>2</sub> and two holes for a TRS and setscrew. On

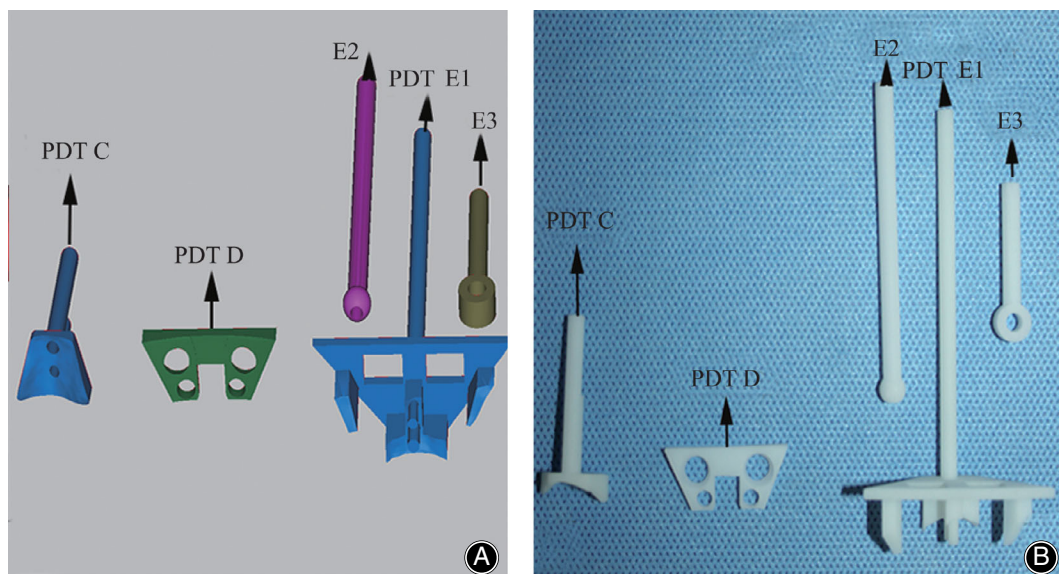


**Fig. 3** Grouped PDTs for C<sub>2</sub>TOPI. (A) The design models of PDT C, D, and E. (B) 3D-printed models of PDT C, D, and E.

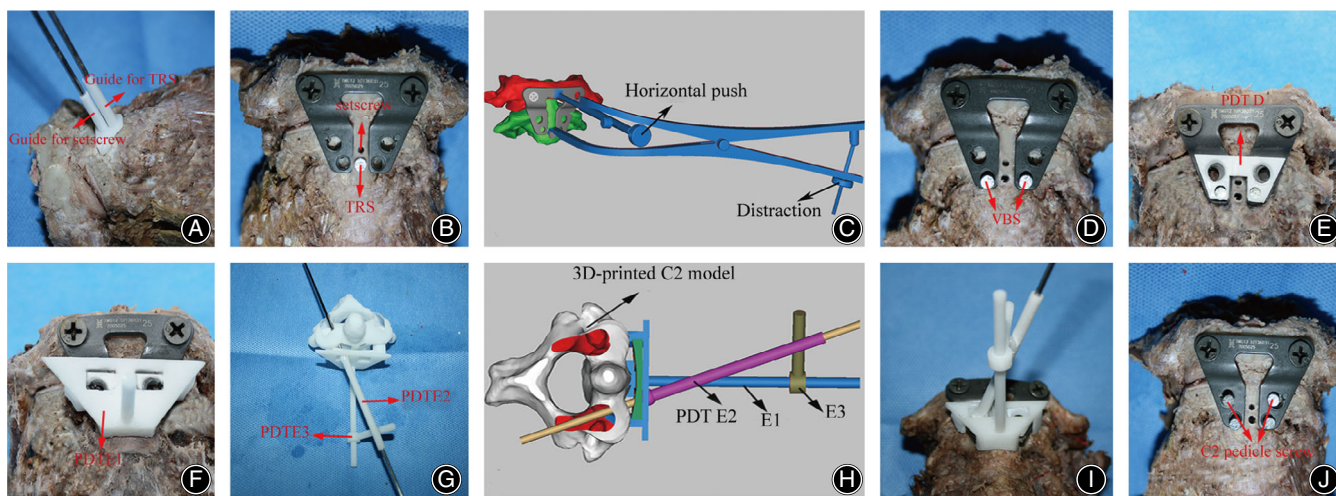


**Fig. 4** Cadaveric C<sub>2</sub>TOPI with the assistance of PDT C, D, and E. (A) PDT C was used to guide the insertions of the TRS and setscrew. (B) A TRS was then screwed in the lower hole, and the upper two holes of the TARP were fixed to C<sub>1</sub> with lateral mass screws. (C) After the TRS was screwed in, C<sub>1</sub> and C<sub>2</sub> were relocated to a proper position with the reduction instrument because it might not obtain the complete reduction (surgical simulation diagrams). (D) The TARP was then temporarily fixed with VBSs. (E) PDT D was used to find the intraoperative position of the TARP according to the positions of the VBSs. The entrance points of C<sub>2</sub>TOPI were determined. (F) After removing the TRS, PDT E1 was attached to the anterior surface of C<sub>2</sub>, and the relative position between PDT D and E1 was agglutinated with a medical glue. (G) PDT D and E1 were transferred to the 3D-printed C<sub>2</sub> model to determine the drilling direction through visual observation. A K-wire was inserted into the pedicle through the drilling tube (PDT E2). The position of the K-wire was adjusted through visual observation to locate it at the central C<sub>2</sub> pedicle. The removable components of PDT E1, E2, and E3 were agglutinated together using the same medical glue to determine the drill direction. (H) Simulation diagrams which showed PDT E1, E2, and E3 were agglutinated to determine the drilling direction. (I) PDT D and E were switched back to the cervical specimen to guide C<sub>2</sub>TOPI with the determined entrance point and drilling direction. (J) C<sub>2</sub>TOPI was completed after the two 3.5-mm diameter screws were inserted.

the table, three removable components (E1, E2, and E3) were designed to guide the K-wire insertion when they were immobilized. These PDTs were created using the same 3D-printing technique described above (Fig. 3B).

### **Cadaver for C<sub>2</sub>TOPI**

The 10 cadavers were operated on by an attending spinal surgeon with either the PDT-guided or freehand technique in random order. The anterior surfaces of C<sub>1</sub> and C<sub>2</sub> were exposed and the soft tissues were removed until the bony surface could be clearly observed. Then the transverse ligament and other soft tissues around the odontoid were resected to create simulated AADs between C<sub>1</sub> and C<sub>2</sub>. In the PDT group, PDT C was placed on the anterior surface of C<sub>2</sub> until a lock-and-key configuration was achieved. K-Wires were then inserted to drill the holes for TRS and setscrew through the two guide tubes of PDT C (Fig. 4A). A TRS was then screwed in the lower hole, and the upper two holes of the TARP were fixed to C<sub>1</sub> with lateral mass screws (Fig. 4B). After the TRS was screwed in, C<sub>1</sub> and C<sub>2</sub> were relocated to a proper position with the reduction instrument because it might not obtain the complete reduction (Fig. 4C). VBSs were then screwed in for temporary fixation of the TARP (Fig. 4D). PDT D was used to find the intraoperative TARP position according to the positions of the VBSs. Thus, the C<sub>2</sub>TOPI entrance points were determined (Fig. 4E). After removing the TRS, PDT E1 was then assembled to attach to the anterior surface of C<sub>2</sub> that was not covered by the TARP. The relative position between PDT D and E1 was agglutinated with a medical glue (COMPONT<sup>®</sup>, Beijing Compont Medical Devices Co., Ltd., Beijing, China), which is a synthetic cyanoacrylic glue that contains the n-butyl-2-cyanoacrylate formulation and is approved by the China Food and Drug Administration (CFDA) as a Class III medical device (Fig. 4F). PDT D and E1 were transferred to the 3D-printed C<sub>2</sub> model to determine the drilling direction. A K-wire was inserted into the pedicle through the drilling tube (PDT E2). The position of the K-wire was adjusted through visual observation to locate it at the central C<sub>2</sub> pedicle. The removable components of PDT E1, E2, and E3 were then agglutinated together using the same medical glue (COMPONT<sup>®</sup>) to determine the drill direction (Fig. 4G,H). PDT D and E were switched back to the cervical specimen to guide C<sub>2</sub>TOPI with the determined entrance point and drill direction (Fig. 4I). C<sub>2</sub>TOPI was completed after the two 3.5-mm diameter screws (Kangli Orthopedic Instrument, Jiangsu, China) were inserted (Fig. 4J). In the fluoroscopy-guided freehand group, the same attending surgeon performed the C<sub>2</sub>TOPI surgeries, applying the technique described in previous publications<sup>1,14</sup>.

### **Comparison of the Operation Time and Screw Placement Accuracy Between the Two Groups**

The operation time for C<sub>2</sub>TOPI surgeries of both groups were recorded. After C<sub>2</sub>TOPI surgeries, a postoperative CT scan was performed, and 3D reconstructions of the cadaveric

C<sub>2</sub> vertebrae with the inserted screws were created with the same procedures. The screw insertion accuracy assessment was performed using Geomagic Studio 11.0 software. The postoperative centroids of the inserted screw at the midpoint of the pedicle in both the PDT and freehand groups were extracted. There were two assessment standards used to evaluate the insertion accuracy: one of the standards was the deviations of the centroids on the axial and sagittal planes of the pedicle between the preoperative design and postoperative screw position. The axial plane deviations towards the lateral side were recorded as positive values, and the deviations towards the medial side were recorded as negative values. The sagittal plane deviations towards the superior and inferior sides were recorded as positive and negative values, respectively. Another intuitive assessment criterion was the grade of the pedicle screw insertion position, which were graded according to the modified All India Institute of Medical Sciences outcome-based classification<sup>18</sup>:

Type I: ideal placement—screw threads are completely within the bony cortex.

Type II: acceptable placement—less than 50% of the diameter of the screw violates the surrounding cortex.

Type III: unacceptable placement—clear violation of the transverse foramen or spinal canal.

### **Statistical Analysis**

The results including the surgery time and deviations are presented as the means  $\pm$  standard deviations. Independent samples *t*-tests were used to analyze the absolute values of the deviations between the two groups on the axial and sagittal planes as well as the surgery time. The chi-square test was performed to compare the pedicle screw position between the two groups. SPSS 20.0 software (IBM Corporation, Armonk, NY, USA) was used for all analyses, and the significance was defined as  $P < 0.05$ .

## **Results**

### **Comparison of the Operation Time Between the PDT and Freehand Groups**

All PDTs were produced successfully using 3D reconstruction and 3D printing. During the operation, the PDTs were fitted to their corresponding anterior cervical surfaces appropriately without any free movement. K-Wires were easily inserted into the cervical pedicle with the assistance of the PDTs. The surgery time was  $47.7 \pm 4.49$  min in the PDT group and  $61.9 \pm 3.21$  min in the freehand group. Compared to the freehand group, the PDT group had a significantly shorter surgery time than the freehand group ( $t = 8.1$ ,  $P < 0.001$ ).

### **Evaluation of the Absolute Deviations from the Centroids Between the PDT and Freehand Groups**

The absolute deviations from the centroids between the preoperative designs and postoperative measurements on the axial plane of the pedicle were  $1.19 \pm 0.25$  mm in the PDT

**TABLE 1** The absolute deviations from the centroids between the preoperative designs and postoperative measurements on the PDT and freehand groups

	PDT group	Freehand group	<i>t</i>	<i>P</i>
Absolute deviations on the axial plane (mm)	1.19 ± 0.25	1.82 ± 0.51	3.42	0.003
Absolute deviations on the sagittal plane (mm)	1.10 ± 0.33	1.70 ± 0.49	3.163	0.006

**TABLE 2** The grade of screw insertion position between the PDT and freehand groups

Grade of screw position	Groups		$\chi^2$	<i>P</i>
	PDT group	Freehand group		
Type I	9 (90%)	5 (50%)	3.651	0.173
Type II	1 (10%)	3 (30%)		
Type III	0	2 (20%)		

group and  $1.82 \pm 0.51$  mm in the freehand group. On the sagittal plane of the pedicle, the corresponding values were  $1.10 \pm 0.33$  mm in the PDT group and  $1.70 \pm 0.49$  mm in the freehand group (Table 1). The absolute deviations of the free-hand group on both the axial and sagittal planes were higher than that of the freehand group ( $t = -3.42$ ,  $P = 0.003$  and  $t = -3.163$ ,  $P = 0.006$ , respectively).

#### Evaluation of the Pedicle Screw Insertion Position Between the PDT and Freehand Groups

For the grade of screw insertion position, there are nine (90%) in type I and one (10%) in type II in the PDT group, whereas there are five (50%) in type I, three (30%) in type II, and two (20%) in type III in the freehand group (Table 2). There were no significant differences between the two groups ( $\chi^2 = 3.651$ ,  $P = 0.173$ ).

#### Discussion

It is well-known that intraoperative reduction of AAD can be divided into complete and incomplete reductions, which require different strategies for PDT design in assisting C<sub>2</sub>TOPI. For AAD with complete reduction, Li *et al.*<sup>19</sup> developed grouped PDTs in their cadaveric study, in which several graded screw trajectories were pre-set to facilitate C<sub>2</sub>TOPI. However, the operation of these PDTs in assisting C<sub>2</sub>TOPI were complex. Therefore, we simplified the design strategy of PDTs and developed an easy-to-apply grouping of preoperative-trajectory-determined PDTs in our previous study<sup>18</sup>. These PDTs have been proved to provide surgeons with an accurate and easy-to-apply method to facilitate C<sub>2</sub>TOPI. However, for AAD with incomplete reduction, to our best knowledge, there has been no report on C<sub>2</sub>TOPI using 3D-printed templates. Therefore, in the present study, we firstly developed a novel intraoperative trajectory-determined strategy of grouped PDTs specifically for

C<sub>2</sub>TOPI in AAD with incomplete reduction, and the efficiency and veracity were validated and compared with those of the fluoroscopy-guided freehand technique.

#### PDTs for C<sub>2</sub>TOPI for AAD with Incomplete Reduction

For AAD with complete reduction, the ideal trajectory of C<sub>2</sub>TOPI that is considered to not only take into account screw insertion safety but also biomechanical properties could be preoperatively designed for this procedure. But in this study, we primarily focused on achieving a safe trajectory of C<sub>2</sub>TOPI for AAD with incomplete anatomical reduction because the trajectories of C<sub>2</sub>TOPI can be determined only after intraoperative reduction. A PDT might be subsequently developed to facilitate C<sub>2</sub>TOPI. However, due to the coverage of the C<sub>2</sub> anterior surface by the TARP after incomplete reduction of AAD, and the various relative positions among C<sub>1</sub>, C<sub>2</sub>, and the TARP, the usual structures of PDTs which determined the trajectories preoperatively and were created using an inverse massive bone surface were not feasible for AAD with incomplete reduction<sup>20-22</sup>. A novel intraoperative trajectory-determined strategy of grouped PDTs for C<sub>2</sub>TOPI was developed. There were three steps in facilitating C<sub>2</sub>TOPI with the PDT. The first step was to facilitate an intraoperative reduction that allowed a TRS, setscrew, and PDT E to find the preoperatively designed positions. PDT C was designed for this step and allowed the determination of the two hole positions for the TRS and setscrew, which were also aligned to the two short pins of PDT E. The second step was to facilitate the location of the entry point of C<sub>2</sub>TOPI after the reduction, which is located at the centre of the pedicle screw holes of the TARP. The determined TARP, including the inferior two holes for VBSs and the central two holes for C<sub>2</sub>TOPI entrances, were used for the location registration. PDT D, which included the inferior two holes and the upper two holes, was specifically designed. PDT D was firmly attached to the anterior surface of the TARP, with good surface registration between the holes. The entry point of C<sub>2</sub>TOPI was then successfully determined. The last step was to facilitate the trajectory drilling of C<sub>2</sub>TOPI. PDT E was designed, which included a table, the beneath registration columns/pins and three above removable components (E1, E2, and E3). The table and the beneath registration columns/pins were the same as those of PDT B in our previous study<sup>18</sup>, and the three above removable components were used to obtain the drill direction of C<sub>2</sub>TOPI. When the K-wire through the removable drilling tube was located at the central pedicle of the 3D-printed C<sub>2</sub> model, the removable

components were then agglutinated together to determine the drilling direction. Then, the entry point and drilling direction of C<sub>2</sub>TOPI were locked by the combined PDTs to allow drilling with a safe trajectory.

### Efficiency and Accuracy of PDTs in Facilitating C<sub>2</sub>TOPI

To ensure the efficiency and accuracy of PDTs in facilitating C<sub>2</sub>TOPI, in the present study, we applied the same means that were used to evaluate the outcome of PDT for AAD with complete reduction<sup>18</sup>. To show the efficiency of PDTs, we calculated the surgery time of the two groups. The surgery time of the PDT group was much shorter than that of the freehand group when performed by the same surgeon, which revealed that the use of a PDT could improve the efficiency of surgeons to facilitate C<sub>2</sub>TOPI. The accuracy of PDTs in facilitating C<sub>2</sub>TOPI is also of vital importance, and two assessment standards were used to evaluate the insertion accuracy: one of the standards was the absolute value of the deviations from the centroids between the preoperative designs and postoperative measurements, which was used to show the actual deviations. Our study showed that the absolute deviations in the axial plane ( $1.19 \pm 0.25$  mm) and the sagittal plane ( $1.10 \pm 0.33$  mm) in the PDT group might be within an acceptable range for clinical application. These results were both significantly different from those in the freehand group. Another intuitive assessment criterion was the critical condition of the cortex being penetrated, which was evaluated by a rank index of the screw insertion position. In our study, no significant difference was observed in the screw positions between the two groups. However, two unacceptable breaches (type III) occurred in the freehand group. This rate was the same as in our previous report (20%)<sup>18</sup> and slightly higher than that in previous reports by

Li *et al.*<sup>14</sup> (13.0%). This result most likely occurred because the surgeon was only an attending spinal surgeon with minimal experience in C<sub>2</sub>TOPI, and the sample size was relatively small. Generally, the results including the surgery time, quantitative absolute values of the deviations and intuitive rank revealed that the PDT-guided technique was more efficient and precise than the fluoroscopy-guided freehand technique in facilitating C<sub>2</sub>TOPI.

### Limitations

Although the novel PDT strategy has obvious advantages in facilitating C<sub>2</sub>TOPI, some limitations need more attention. First, these PDTs were mainly applied for simple atlantoaxial dislocation with relatively intact bony structure. For the patients with anterior C<sub>2</sub> fracture, these PDTs cannot fit well to the fractured surface of C<sub>2</sub>, thus limiting its clinical application<sup>23</sup>. Second, the placement of the group PDTs and the reduction instruments were demonstrably difficult in terms of transoral accessibility in a deep surgical field, and the cadaveric simulation experiment did not fully represent the relevant intraoperative situation. Therefore, the aim of this study was only to introduce a novel technical strategy of the PDTs for AAD with incomplete reduction and to further evaluate the efficiency and accuracy of PDTs in facilitating C<sub>2</sub>TOPI. Further improvements can be made in clinical applications, depending on the actual situation.

### Conclusion

In summary, the novel intraoperative trajectory-determined strategy of grouped PDTs could be used as an accurate and feasible method for C<sub>2</sub>TOPI for AAD with incomplete reduction. This could provide a viable alternative for surgeons.

## References

1. Yin Q, Li X, Bai Z, *et al.* An 11-year review of the TARP procedure in the treatment of Atlantoaxial dislocation. *Spine (Phila Pa 1976)*, 2016, 41: E1151–E1158.
2. Zhu C, Wang J, Wu Z, Ma X, Ai F, Xia H. Management of pediatric patients with irreducible atlantoaxial dislocation: transoral anterior release, reduction, and fixation. *J Neurosurg Pediatr*, 2019, 14: 1–7.
3. Xu J, Yin Q, Xia H, *et al.* New clinical classification system for atlantoaxial dislocation. *Orthopedics*, 2013, 36: e95–e100.
4. Yin Q, Ai F, Zhang K, Mai X, Xia H, Wu Z. Transoral atlantoaxial reduction plate internal fixation for the treatment of irreducible atlantoaxial dislocation: a 2- to 4-year follow-up. *Orthop Surg*, 2010, 2: 149–155.
5. Lan S, Xu J, Wu Z, *et al.* Atlantoaxial joint distraction for the treatment of basilar invagination: clinical outcomes and radiographic evaluation. *World Neurosurg*, 2018, 111: e135–e141.
6. Ai F, Yin Q, Xu D, Xia H, Wu Z, Mai X. Transoral Atlantoaxial reduction plate internal fixation with Transoral Transpedicular or articular mass screw of C2 for the treatment of irreducible. *Atlantoaxial Dislocation Spine*, 2011, 36: E556–E562.
7. Xu R, Kang A, Ebraheim NA, Yeasting RA. Anatomic relation between the cervical pedicle and the adjacent neural structures. *Spine (Phila Pa 1976)*, 1999, 24: 451–454.
8. Bydon M, Mathios D, Macki M, *et al.* Accuracy of C2 pedicle screw placement using the anatomic freehand technique. *Clin Neurol Neurosurg*, 2014, 125: 24–27.
9. Sciuabba DM, Noggle JC, Vellimana AK, *et al.* Radiographic and clinical evaluation of free-hand placement of C-2 pedicle screws. *J Neurosurg Spine*, 2009, 11: 15–22.
10. Yeom JS, Buchowski JM, Park KW, Chang BS, Lee CK, Riew KD. Undetected vertebral artery groove and foramen violations during C1 lateral mass and C2 pedicle screw placement. *Spine (Phila Pa 1976)*, 2008, 33: E942–E949.
11. Ondra SL, Marzouk S, Ganju A, Morrison T, Koski T. Safety and efficacy of C2 pedicle screws placed with anatomic and lateral C-arm guidance. *Spine (Phila Pa 1976)*, 2006, 31: E263–E267.
12. Tessitore E, Bartoli A, Schaller K, Payer M. Accuracy of freehand fluoroscopy-guided placement of C1 lateral mass and C2 isthmus screws in atlanto-axial instability. *Acta Neurochir*, 2011, 153: 1417–1425.
13. Yang YL, Zhou DS, He JL. Comparison of isocentric C-arm 3-dimensional navigation and conventional fluoroscopy for C1 lateral mass and C2 pedicle screw placement for atlantoaxial instability. *J Spinal Disord Tech*, 2013, 26: 127–134.
14. Li X, Ai F, Xia H, Wu Z, Ma X, Yin Q. Radiographic and clinical assessment on the accuracy and complications of C1 anterior lateral mass and C2 anterior pedicle screw placement in the TARP-III procedure: a study of 106 patients. *Eur Spine J*, 2014, 23: 1712–1719.
15. Tian W, Weng C, Liu B, *et al.* Posterior fixation and fusion of unstable Hangman's fracture by using intraoperative three-dimensional fluoroscopy-based navigation. *Eur Spine J*, 2012, 21: 863–871.
16. Yu X, Li L, Wang P, Yin Y, Bu B, Zhou D. Intraoperative computed tomography with an integrated navigation system in stabilization surgery for complex craniovertebral junction malformation. *J Spinal Disord Tech*, 2014, 27: 245–252.
17. Liu G, Buchowski JM, Shen H, Yeom JS, Riew KD. The feasibility of microscope-assisted "free-hand" C1 lateral mass screw insertion without fluoroscopy. *Spine (Phila Pa 1976)*, 2008, 33: 1042–1049.
18. Lin L, Zhu M, Peng P, Zhang X, Zhou X, Li J. Patient-specific drill template for C2 transoral pedicle insertion in complete reduction of atlantoaxial

dislocation: cadaveric efficacy and accuracy assessments. *J Orthop Surg Res*, 2019, 14: 141.

**19.** Li XS, Wu ZH, Xia H, *et al.* The development and evaluation of individualized templates to assist transoral C2 articular mass or transpedicular screw placement in TARP-IV procedures: adult cadaver specimen study. *Clinics*, 2014, 69: 750–757.

**20.** Lu S, Xu YQ, Chen GP, *et al.* Efficacy and accuracy of a novel rapid prototyping drill template for cervical pedicle screw placement. *Comput Aided Surg*, 2011, 16: 240–248.

**21.** Berry E, Cuppone M, Porada S, *et al.* Personalised image-based templates for intra-operative guidance. *Proc Inst Mech Eng H*, 2005, 219: 111–118.

**22.** Fu M, Lin L, Kong X, *et al.* Construction and accuracy assessment of patient-specific biocompatible drill template for cervical anterior transpedicular screw (ATPS) insertion: an in vitro study. *PLoS One*, 2013, 8: e53580.

**23.** Wu X, Liu R, Xu S, *et al.* Feasibility of mixed reality-based intraoperative three-dimensional image-guided navigation for atlanto-axial pedicle screw placement. *Proc Inst Mech Eng, Part H*, 2019, 233: 1310–1317.